УДК 539.4
EDN LJSDEA (https://elibrary.ru/ljsdea)
DOI 10.33113/mkmk.ras.2023.29.02.04

EXPERIMENTAL STUDY AND NUMERICAL ANALYSIS OF THE EFFECT OF TEMPERATURE ON DAMAGED AND NOTCHED COMPOSITE PLATES REPAIRED WITH COMPOSITE MATERIALS UNDER THERMAL LOADING

Berrahou Mohamed, Belkadour Leila

University of Relizane, Relizane, Algeria

ABSTRACT

This research presents the results of an experimental and analytical program to study the effect of thermal loading on the mechanical properties of the most commonly used composite materials at present temps in the market, as well as the effect of the stacking sequence and fiber orientations on the hardness of these materials under different temperatures (room temperature (~20°C) and their elevation to extreme temperatures 40, 60, 80, 100°C). In this sense, this study was conducted in two phases: the first is an experimental study that includes practical tests on the tensile strength of several types of composites at different temperatures, in addition to tests on different fibers orientations under different thermal loads. As for the second study, it is an analytical study using the ABAQUS program, related to the analysis of the thermal effect on stress intensity factor (SIF), stress concentration factor (SCF), and the stresses distribution for different stacking sequences. The conclusion drawn from both studies is that the general mechanical properties of composite materials decrease with increasing temperature, as these materials are negatively affected by increasing temperature.

Keywords: composite; ultimate strength σ_u; stress intensity factor (SIF); stress concentration factor (SCF); von Mises Stress

1. INTRODUCTION

The field of use of repairs and reinforcements with composite materials has been expanded in recent years, due to its advantages and excellent properties compared to traditional materials used, especially in the fields of aviation, marine and aerospace, such as higher strength and toughness to weight ratio, improved wear, environmental resistance, design flexibility, improved fatigue life, and potential reduction in processing, manufacturing and life cycle cost [1,2]. The selection of composite materials for the target repair is based on the initial performance and functional expectations of the repaired structure, as well as the maintenance of this performance throughout the service life. However, these materials also have their drawbacks and disadvantages that are now areas of recent research and studies. Among these axes are the wear and corrosion of composites and the effect of stacking sequences and fiber orientations on the toughness of repairs [3].

The temperature has a great influence on the behavior and performance of composite materials. Some researchers have investigated the effects of temperature on the composites mechanical properties. There is a study conducted by researcher Soutis and Turkmen in which they analyzed the effects of humidity and temperature on compressive strength and failure of unidirectional glass-polypropylene laminated

plates. One of their most important observations is that sample failure always occurs as a result of precise out-of-plane micro buckling. This is due to the decrease in the strength of the matrix with increasing temperature, which confirms the effect of this phenomenon on the behavior of composite materials [4]. In addition to, an experimental study of the compressive failure of carbon-epoxy laminated plates at high temperatures between 20 and 100^{o}C, using untabbed specimens, and proved that there is no damage to the surface layers. Sample preparation costs are greatly reduced due to the unrestricted tabs performed by Soutis et al. [5]. El-Hawary and Abdel-Fattah [6] studied the compressive strength, tensile strength, stiffness, modulus of elasticity and stress-strain relationships under repeated loading of resin concrete cylinders prepared using different types of resins such as epoxy and polyester, and at different rates in four different temperature stations ranging from room temperature 20^{o}C to the maximum possible degree in reality 200^{o}C. From the test results, it is evident that the compressive strength increases with increasing temperature and the amount of epoxy. The same results were obtained for the hardness of polymer concrete. By increasing the temperature, the modulus of elasticity does not change significantly, while the tensile strength decreases.

In addition to all these studies, studies on the behavior of composite materials under high and elevated temperatures have been conducted. However, glass-carbon and carbon-glass composite laminates have shown poor mechanical behavior under high and elevated temperatures and may reduce the life of structures designed using these materials [7-10]. When the working temperatures of the structures are above the glass transition temperatures (Tg) of the matrix, the materials become softer and may collapse [11]. The elevated temperature may be attributed to chemical and/or physical damages caused by the polymer matrix, loss of adhesion at the fiber/matrix interface, and/or reduced strength and stiffness of the fibers [12]. The thermal effect on composites has been carefully studied, according to [13] the higher the temperature, the more significantly the mechanical properties of the composites are modified, the distribution of stress concentrations can then be varied, highlighting several potential damage states. Compounds are generally sensitive to thermal effects, and these effects have reduced the mechanical strength of the composite material, affecting the repair efficiency [14].

The focus of this study is the effect of fibers orientation of composite materials under thermal influence on the general behavior of the composite [15]. The geometric arrangement of the fibers and their shapes can cause significant anisotropy. In this sense, Benkhira [16] conducted a study on improving the shape of the composite patch. An experimental study of the mechanical behavior of a fiber-reinforced composite plate was performed by Vu et al. [17] in order to study the assembly of a composite plate. In addition, in [18] the effect of sheet fiber length and fragmentation size on the mechanical behavior of plates was examined.

The analytical results of a study by [19] showed that the assumption of 2-D fiber random orientation is suitable for unreinforced ultra-high-performance fiber-reinforced concrete beam (UHPFRC**)**, while 3-D random fiber orientation assumption is suitable to reinforce with steel, UHPFRC beams and glass fiber-reinforced polymer (GFRP) rebar due to fiber alignment disturbance from internal reinforcements. [20] evaluated the effect of residual stresses from fabrication of imperfect surfaces on stress crack growth in nickel-based super alloys. The performance of the repair depends on the method of assembly between the substrate and the repair patch. Recent literature has studied stress concentration factor changes around cracks to avoid their propagation [21,22]. SIF (stress intensity factor) depends on many parameters such as mechanical

properties of materials, type of loading, size and geometry of the structure. In addition to all these studies, the researcher Berrahou Mohamed with a group of researchers in a laboratory at the University of Sidi Bel Abbes in Algeria studied the thermal effect on the cracked and corroded plate using the ABAQUS program, where they proved that the adhesives are subject to deterioration under the thermal effect during service [23].

This paper aims to study the effect of temperature on the deterioration of the mechanical behavior of unidirectional composite plates. The static mechanical properties of the composite films were determined at different temperatures ranging from room temperature 20°C to high temperatures of up to 100°C. In this work, two methods of analysis were used, the first is the experimental method which depends on studying the effect of heat on the ultimate strength of the composite material damage according to different fiber directions of the composite plates, and on the hardness of the plates of different types of supple and stiff repairs. The second method is numerical analyzes using the ABAQUS program, where we analyzed the thermal effect on the stress intensity factor SIF, the stress concentration factor SCF, and the Von Mises stress with respect to the different stacking sequence.

2. GEOMETRICAL MODEL

We consider a notched and cracked rectangular plate made of various types of composite materials (Boron/epoxy, graphite/epoxy, glass/epoxy) with the following dimensions (height $H = 204$ mm, width $W = 152$ mm and thickness $E\_P = 3.2$ mm) containing a V-shaped cut having the following dimensions: (radius $r = 15.2$ mm, $b = 23.8$ mm), The plate was repaired with a simple composite patch (Boron/epoxy) of constant thickness $e_{pa} = 1.6$ mm. In order to analyze the effect of patch shape, three patch geometries were chosen in this study: (A) total, (B) normal and (C) V-shaped, this patches and model of the structure shown in fig.1. The patch is glued with 0.127 mm thick adhesive. The structure composed of the plate is stressed by uniaxial traction $\sigma = 120$ MPa.

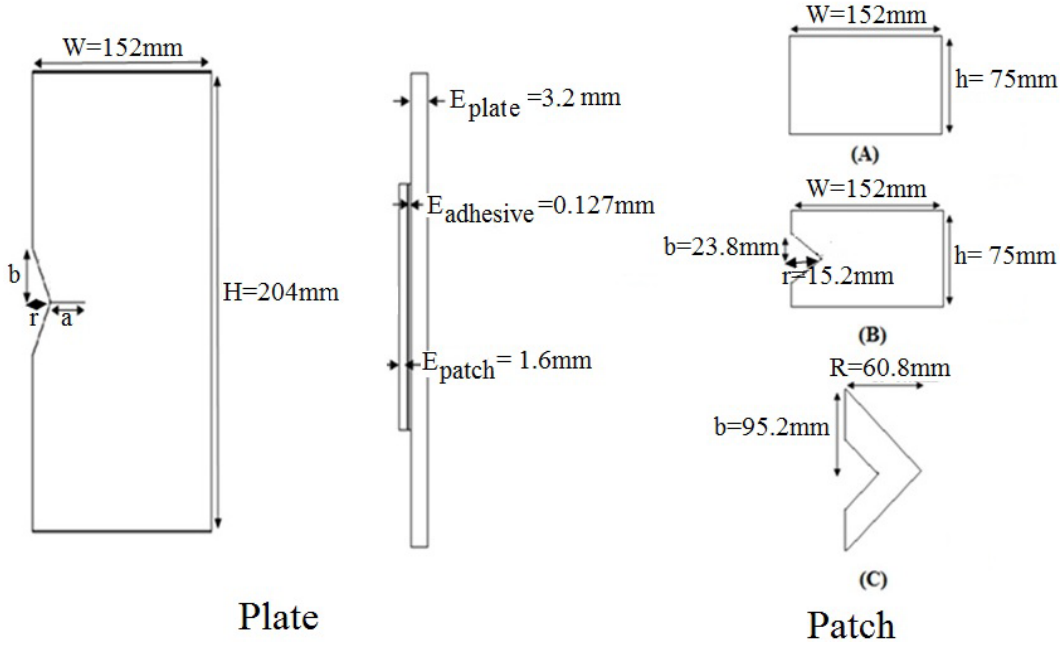

Fig.1. Geometric model of structure and for (total, normal and V) patch shape.

The mechanical properties of the different types of materials are given in Table 1 below.

Table 1.

Mechanical properties of different materials [22].

Description	boron/epoxy	graphite/ epoxy	glass/epoxy	Adhesive (FM73)
Young's modulus in X direction (GPa) E_1	200	127.5	50	2.550
Young's modulus in Y direction (GPa) E_2	19.6	9.00	25	
Young's modulus in Z direction (GPa) E_3	19.6	4.80	25	
Poisson's Ratio in X-Y plan υ_{12}	0.3	0.342	0.21	0.32
Poisson's Ratio in X-Z plan υ_{13}	0.28	0.342	0.21	
Poisson's Ratio in Y-Z plan υ_{23}	0.28	0.38	0.21	
Shear modulus in X-Y plan (GPa) G_{12}	7.2	4.8	7.2	
Shear modulus in X-Z plan (GPa) G_{13}	5.5	4.8	5.5	
Shear modulus in Y-Z plan (GPa) G_{23}	5.5	2.55	5.5	

3. RESULTS AND DISCUSSION

This study relied on two aspects, an experimental and numerical analysis aspect, and then a comparison between their results. In both sides we wanted to study the effect of heat on the behavior of composite plates.

In the first part, we chose a V-shaped composite plate repaired with several types of composite (boron / epoxy, graphite / epoxy and glass / epoxy) with the stacking sequence [0/45/-45/90] seconds. This panel is subjected to a pure tension of $\sigma = 120$ Pa to study the maximum failure strength, as well as the effect of thermal effect on the mechanical properties of the composite plates.

3.1. Experimental Part.

The recent literature shows that the performance of repairs based on the technology of composite materials depends not only on the rigidity, but also on the stacking sequence and fiber directions of the structures and the effect of loading, whether mechanical or thermal. For this reason, this stage has been divided into two parts.

The first stage is aimed at evaluating the ultimate strength of failure on the plate made of several types of composite (boron/epoxy, graphite/epoxy and glass/epoxy), with a V-shaped notch is shown in fig.2.

The considered compound consists of a uniform fiber direction [0/45/-45/90]s, which makes it possible to focus only on thermal stress to choose the compound with

the best tear resistance and resistance to thermal loads. In the second phase, we analyze the thermal effect on the elastic properties of the same composite plates.

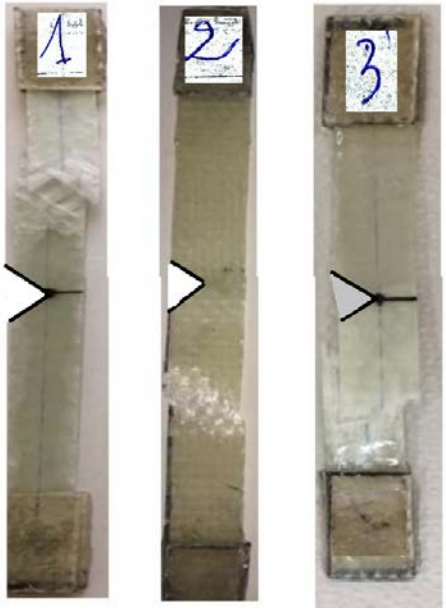

Fig.2. Composite plates: (1) boron / epoxy, (2) glass / epoxy and (3) graphite / epoxy.

3.1.1. Ultimate strength of the failure of different composites types for ambient temperature T=20ºC.

According to fig.3, we can see that the longitudinal direction of graphite/epoxy has the best resistance to rupture since its maximum stress is the highest (800 MPa) by a rate of 50% compared to the other types of composites.

For the transverse direction, the failure strength was reduced to half of the longitudinal direction (Θ=0°). The maximum stress was at 220 MPa, that of graphite/epoxy. The other types of composites (boron/epoxy and glass/epoxy) have lower stresses by a rate of 50% less than graphite/epoxy.

For the longitudinal compressive and transverse compressive directions have the same behavior as the two other directions mentioned above. The breaking stress of graphite/epoxy is Twice more efficient compared to other types of composites.

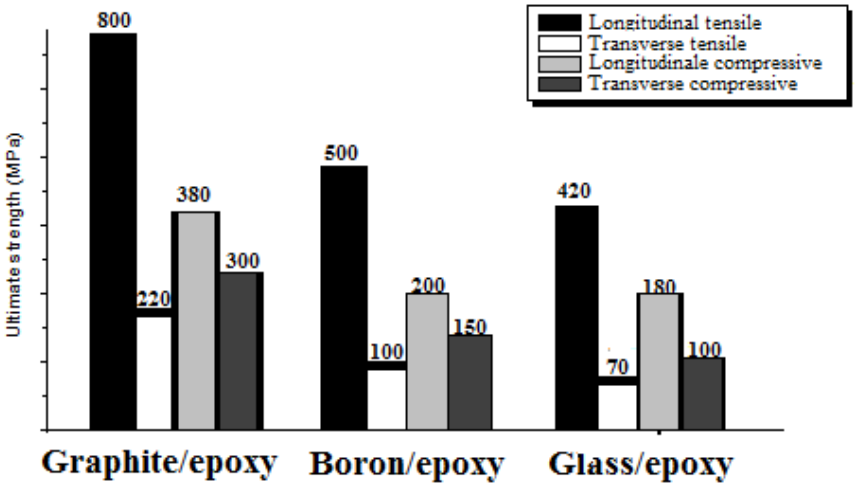

Fig.3. Effect of temperature on the mechanical properties of composite plates.

3.1.2. Study of ultimate strength as a function of temperature for the graphite/epoxy composite.

This study is equipped to evaluate the loss of stiffness during the influence of varying temperatures on composite plates, by accentuating the effect of fiber orientation on the stiffness of laminated composite structures.

Fig.4 shows the variations in ultimate strength as a function of thermal variations for the composite plate type (graphite/epoxy), and for four fiber orientations: longitudinal tensile, transverse tensile, longitudinal compressive and transverse compressive.

The failure strength maintained its value in the vicinity of (800-700) MPa up to 60ºC of temperature for the transverse direction of the fibers, and begins to reduce up to half (50%) at 100ºC.

For the longitudinal compressive direction, the elastic modulus is lower by a rate of 60% than that of the transverse direction of the fibers. But the two other directions of orientation of the remaining fibers practically have very low modulus of elasticity for all the degrees of temperature applied.

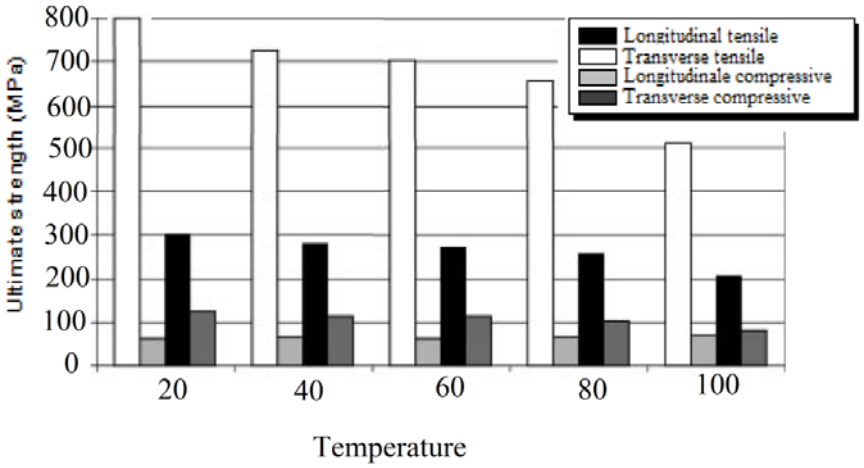

Fig.4. Elastic modulus values as a function of temperature for the graphite/epoxy composite material in several fiber orientations.

3.1.3. Study of laod- displacement as a function of temperature for the graphite/epoxy composite.

Fig.5 shows the effect of heat on the case of a V-notched graphite/epoxy plate. This figure shows the differences in tensile stress with displacement of graphite/epoxy samples at different temperature ranges. After examining the results, it was found that the increase in temperature, especially above 60ºC reduces the efficiency of the composite material, which increases the risk of damage and deterioration of its mechanical properties.

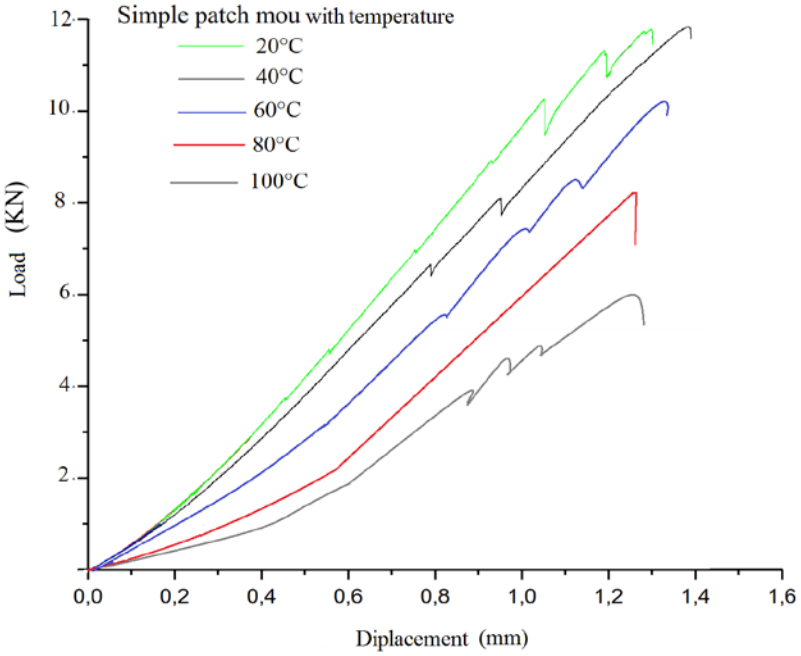

Fig.5. Load-displacement curves as a function of temperature.

3.2. Simulation Part.

In this part, we simulated a plate made of several types of composite with a V-shaped notch repaired by a glass/epoxy patch in several shapes (Total, Normal and U-shaped) glued by FM73 type bonding with a thickness of 127 mm.

3.2.1. Finite element model.

The analysis involves a three-dimensional finite element method using the finite element code ABAQUS [24]. The finite element model is composed of three subsections for a cracked composite plate with a V-shaped notch, the adhesive, and the composite part (patch). The plate has two layers of elements in the thickness direction, the patch and the adhesive had a single layer of elements through the thickness. The mesh model contains 12148 quadratic hexahedral elements of type C3D20R. Total number of nodes is 68829. The size of the side of an element equal to 0.016 mm for the whole structure and 0.004 mm in the vicinity of the notch, the notched plate and the patch as well as the adhesive have a linear elastic behavior. This mesh of the notched and cracked specimen repaired with different shapes of the patches used for the three-dimensional numerical analysis is shown on the fig.6, and the boundary conditions imposed on the plate analyzed are represented as follows in fig.7.

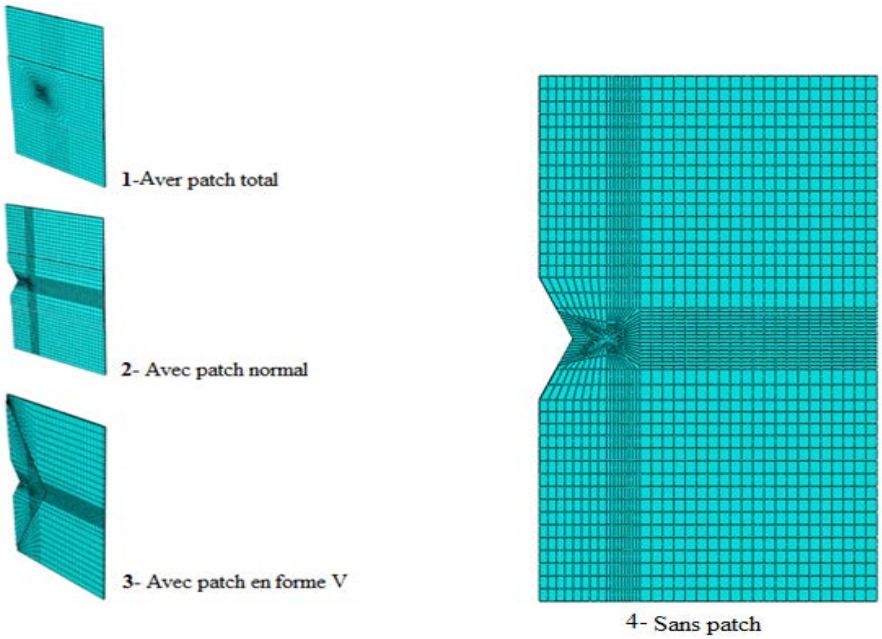

Fig.6. Mesh model.

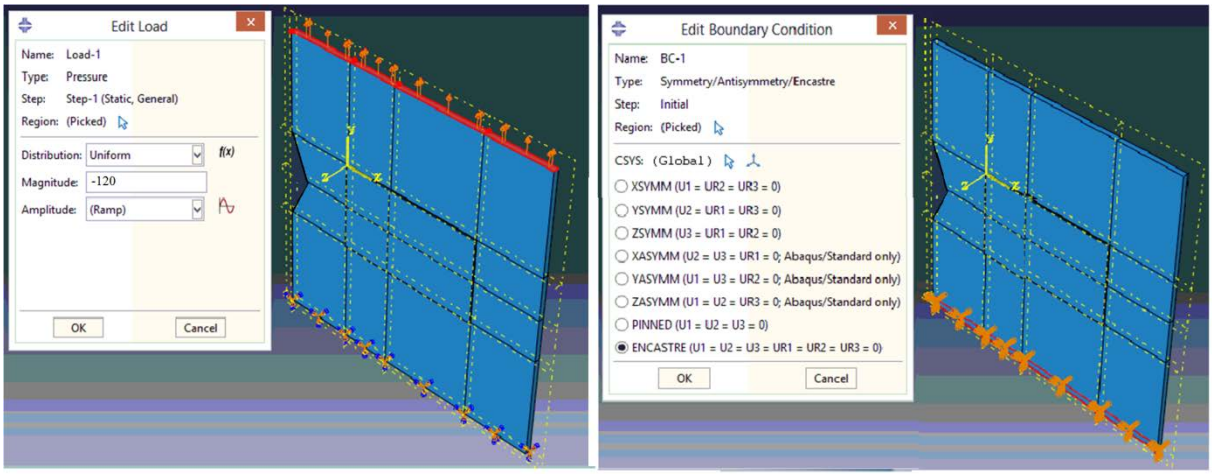

Fig.7. The boundary conditions of the geometrical model.

The lamination of the plate comprises eight $[0/45/-45/90]_S$ stacking sequence plies, the thickness of an elementary ply of which is 0.4 mm. The patch is four folds of sequence [0/45/-45/90]. The thickness of an elementary ply is 0.4 mm (see fig.8).

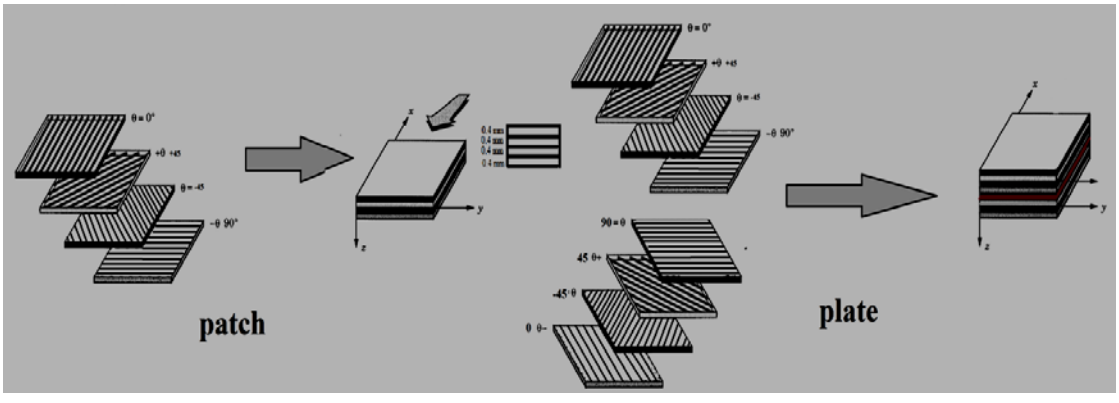

Fig.8. Plies orientation in the patch and plate.

3.2.2. Variation of the damaged zone of adhesive for different type's plates.

We have established this part at the end of recovery of the evolution of the damaged zone in the adhesive layer in FM73 within a V-shaped notched plate in different types of composite materials (Boron / epoxy, Glass / epoxy and Graphite / epoxy) with a longitudinal crack a (mm) repaired with a composite patch (Boron/epoxy) of geometric shape (total, normal, V-shaped). The damaged area theory was used.

The theory's Main assumption of is that the adhesive and crack initiation in the bonded patch occurs after a damaged area develops. Under low amplitude of load, the localized damages arrive at the edges of patch. This damage occurs because the material is locally subjected to strains higher than the ultimate material strain. Under medium load amplitude, the damaged zones grow in size and the concentration of points of the damaged areas increases. As the failure load is reached the damaged area in the adhesive grows to a critical size and the individual components of the damage coalesce and form a crack. Numerically, the damaged area is identified by marking items for which a failure criterion is exceeded. The adhesive tested is a toughened ductile adhesive which is expected to fail in performance. Consequently, the failure criterion used for the cohesive damage of the adhesive layer is the equivalent Von Mises strain criterion

$$\varepsilon_{equiv} = \frac{1}{\sqrt{2(1+\vartheta)}} X \sqrt{\left(\varepsilon_{p1}-\varepsilon_{p2}\right)^2 + \left(\varepsilon_{p2}-\varepsilon_{p3}\right)^2 + \left(\varepsilon_{p3}-\varepsilon_{p2}\right)^2}. \qquad (1)$$

Where ε_{equiv} is the equivalent stain, ε_{pi} are the plastic strains in the different directions and ϑ the Poisson ratio.

This criterion is satisfied when the maximum principal strain in the material reaches the ultimate principal strain. For each failure criterion an ultimate strain will be defined and the corresponding damage zone size at failure is determined. The damaged area theory is based on the principle that the adhesive joint is assumed to fails when the damaged area reaches a certain critical value. The damaged zone can be determined by either a stress or a strain criterion. Therefore, the adhesive fails to perform its functions when the cohesive failure criterion is satisfied the adhesive joint. Since adhesive failure occurs at the adhesive joint, the adhesive failure criterion for the damaged area should be used.

The failure criterion is determined for each stress exerted when it reaches the maximum stress allowed in the material, the area of damage will be determined as the area where the stress of the FM-73 adhesive exceeds 7.87% of the area of damage. Shang Bang after having carried out studies on the FM-73 that the latter no longer provides an adequate function of binder when the value of the DR ratio exceeds 0.24 which considers it as a critical value [25]. The value of the damaged area ratio is calculated according to the following relationship

DR = sum of damaged areas / total adhesive area.

Boron/epoxy plate

Fig.9 represents the results obtained which make it possible to follow the development of the damaged area of the adhesive for a V-notched boron/epoxy composite plate repaired by boron/epoxy patch of shape (gross, normal and V-shaped). It can be seen by following the damaged area, which increases with temperature, especially above T = 60°C (ΔT = 40°C). We note that the damaged area appears very

little around the notch area and increases more with increasing temperature to include the edge area also, for a V-shaped patch.

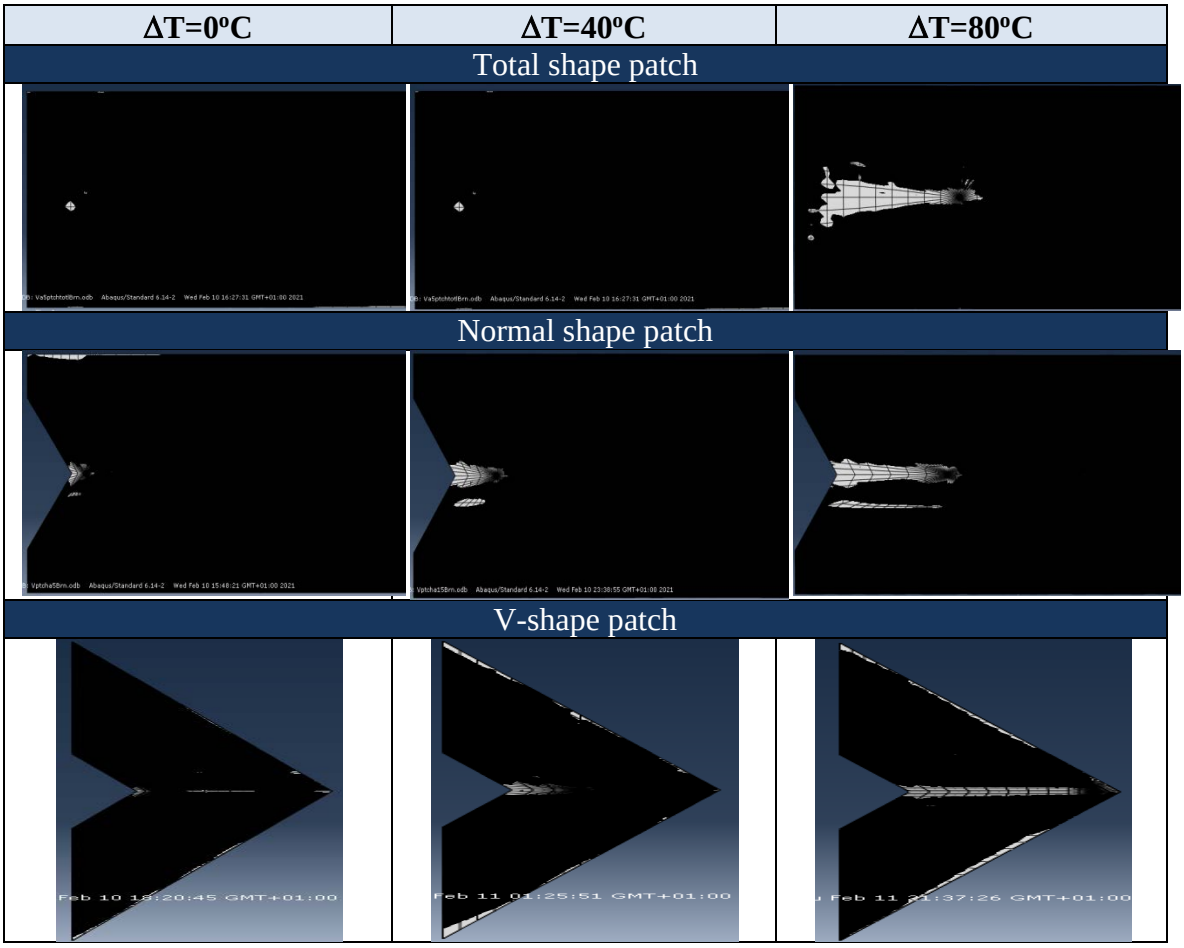

Fig.9. Damaged area of FM73 adhesive vs the temperature for Boron/epoxy plate, patch shape (total, normal, V-shaped).

Graphite/epoxy plate

Fig.10 presents the obtained results that allow following the development of the damaged area of the adhesive for a graphite/epoxy composite plate repaired with a boron/epoxy composite patch with different shapes. It is noted that the appearance of the damaged area increases with increasing temperature, and this increase appears clearly in the vicinity of the notch and at the edges of the patch.

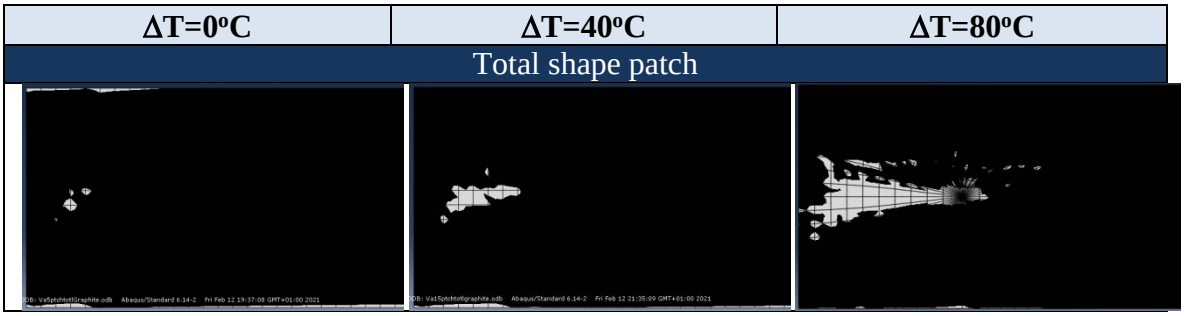

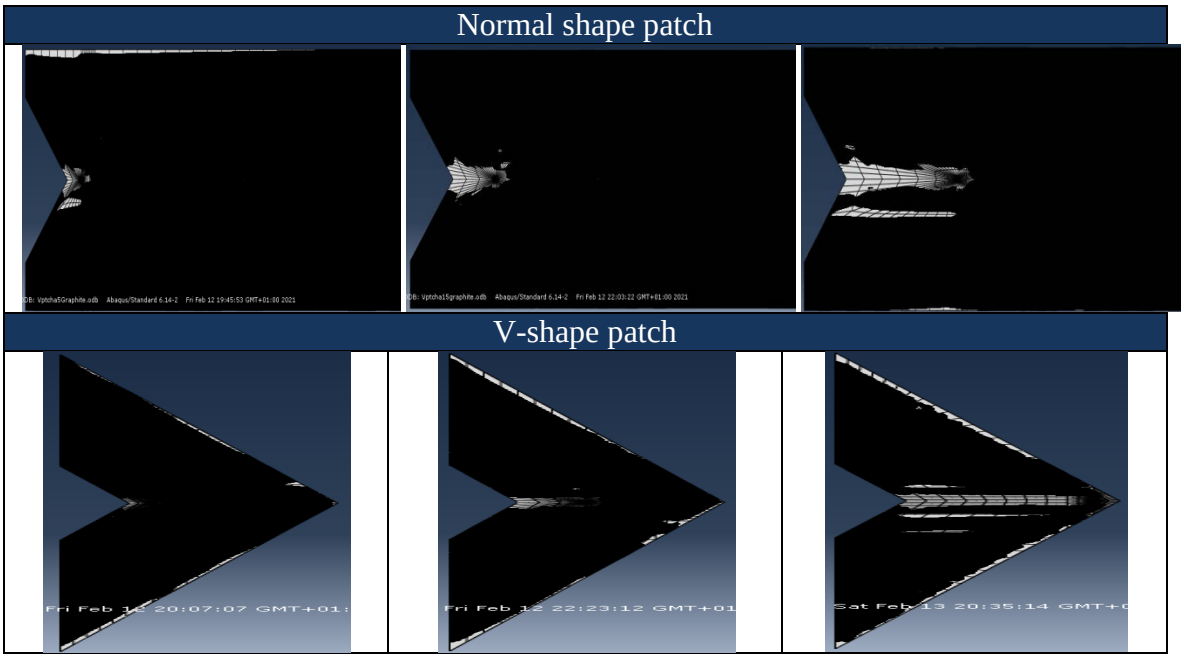

Fig.10. Damaged area of FM73 adhesive vs the temperature for Graphite/epoxy plate, patch shape (total, normal, V-shaped).

Glass/epoxy plate

Fig.11 shows the results obtained for the differences in the damaged area of the adhesive for a glass/epoxy notched plate repaired by boron/epoxy patch and with different shapes (Total, normal and V shaped). It is noted that the damaged area increases with increasing temperature until it reaches its maximum at temperature T = 100^{o}C, where we note that the damaged area includes the notch area and extends to include the area of the edges of the patch for all shapes of the patch.

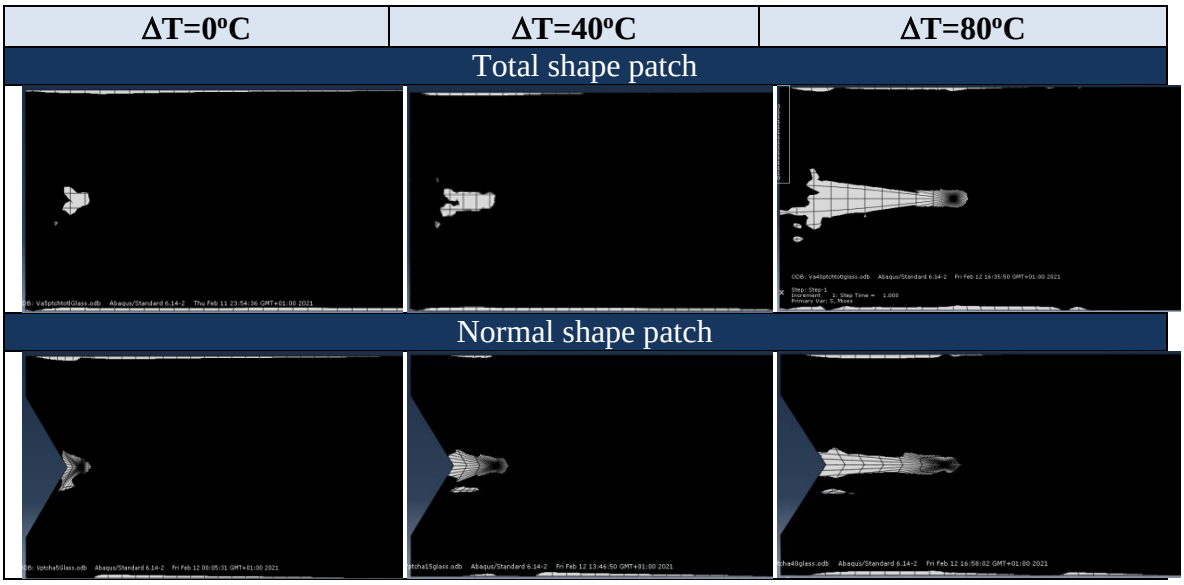

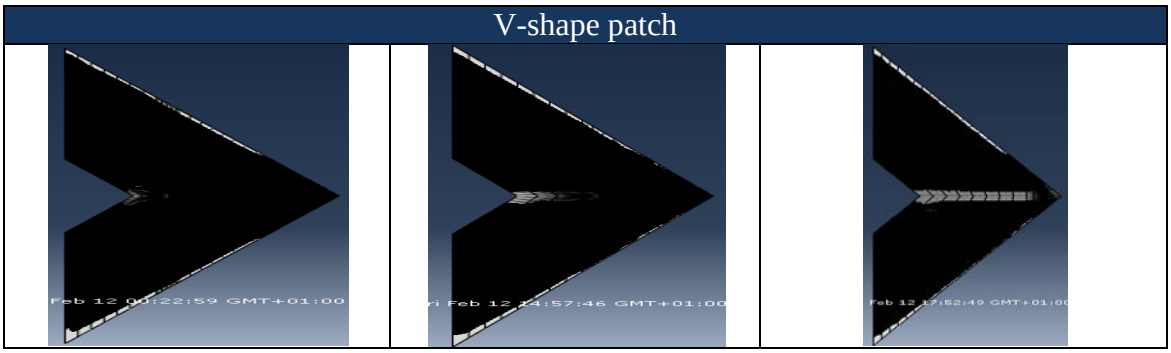

Fig.11. Damaged area of FM73 adhesive vs the temperature for Glass/epoxy plate, patch shape (total, normal, V-shaped).

3.2.3. Variation of the damaged area ratio of the adhesive as a function of temperature for different shapes patch.

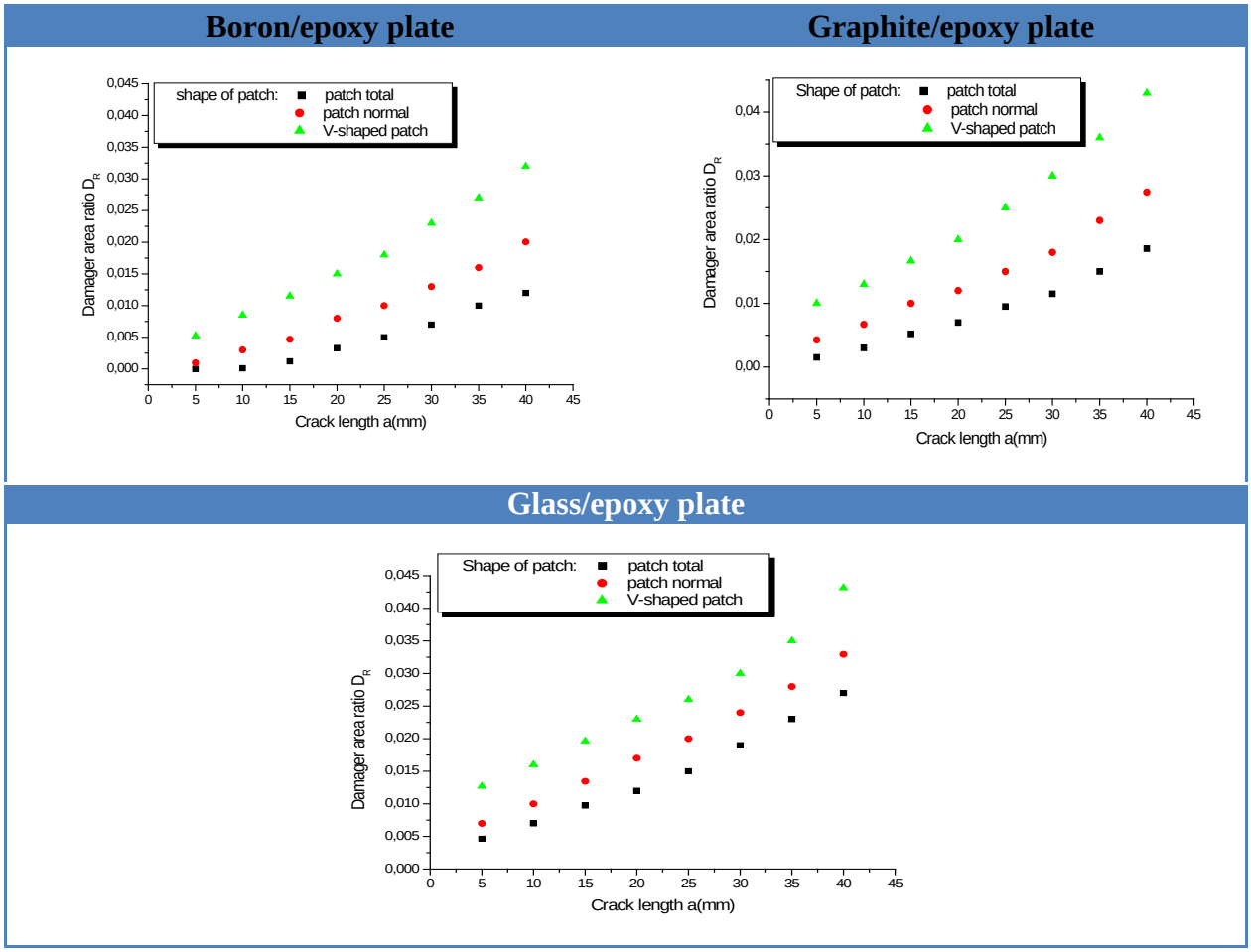

Fig.12. Report of the damaged area D_R for a plate in (Boron/epoxy, Graphite/epoxy and Glass/epoxy) repaired by composite patch of different shapes.

Fig.12 represents the results of calculating the damaged area ratio (DR) according to temperature, for notched plates of different composite materials (boron / epoxy, graphite / epoxy and glass / epoxy), repaired by boron / Epoxy patch for the same FM73 adhesive. The results show that all DR values are less than the critical DR value (0.2474). According to the above curves, it is seen that an increase in temperature leads

to an increase in DR. When comparing the materials used, we saw that boron / epoxy is the most efficient compound because it gives lower DR values than other materials. And we also concluded that the use of the patch with the total shape is more positive compared to the other shapes because it covers and protects all areas of the plate.

3.2.4. Effect of temperature on the stress intensity factor.

The stress intensity factor (SIF) at the crack front was extracted using the virtual crack closure technique (VCCT). The virtual crack closure technique (VCCT) criterion uses the principles of linear elastic fracture mechanics (LEFM) and, therefore, is appropriate for problems in which brittle crack propagation occurs along predefined surfaces. VCCT is based on the assumption that the strain energy released when a crack is extended by a certain amount is the same as the energy required closing the crack by the same amount. The stress intensity factors at the crack tip are calculated using the virtual crack closure technique (VCCT) based on the energy balance. In this technique, the stress intensity factors are obtained for the three failure modes according to the equation

$$G_i = \frac{K_i^2}{E}. \qquad (2)$$

Where G_i is the Fracture energy for mode I, K_I is the stress intensity factor for mode i and E is the modulus of elasticity.

The model referred to above is called the linear elastic fracture mechanics model and has found wide acceptance as a method for determining the resistance of a material to below-yield strength fractures, the model is based on the use of linear elastic stress analysis. Therefore, in using the model one implicitly assumes that at the initiation of fracture any localized plastic deformation is small and considered within the surrounding elastic stress field.

$$\sigma_x = \frac{K}{\sqrt{2\pi r}}\cos\frac{\theta}{2}\left[1-\sin\frac{\theta}{2}\sin\frac{3\theta}{2}\right],$$
$$\sigma_y = \frac{K}{\sqrt{2\pi r}}\cos\frac{\theta}{2}\left[1+\sin\frac{\theta}{2}\sin\frac{3\theta}{2}\right], \qquad (3)$$
$$\sigma_{xy} = \frac{K}{\sqrt{2\pi r}}\sin\frac{\theta}{2}\left[\cos\frac{\theta}{2}\cos\frac{3\theta}{2}\right]/$$

The stress in the third direction are given by $\sigma_z = \sigma_{xz} = \sigma_{yz} = 0$ for the plane stress problem, and when the third directional strains are zero (plane strain problem), the out of plane stresses become $\sigma_{xz} = \sigma_{yz} = 0$, and $\sigma_z = \vartheta\left(\sigma_x + \sigma_y\right)$. While the geometry and loading of a component may change, as long as the crack opens in a direction normal to the crack path, the crack tip stresses are found to be as given by Equations 2.

The stress intensity factor (K) is used in fracture mechanics to predict the stress state "stress intensity" near the tip of a crack or notch caused by a remote load or residual stresses. It is a theoretical construct usually applied to a homogeneous, linear elastic material and is useful for providing a failure criterion for brittle materials, and is a critical technique in the discipline of damage tolerance. The concept can also be applied to materials that exhibit small-scale yielding at a crack tip.

The magnitude of K depends on specimen geometry, the size and location of the crack or notch, and the magnitude and the distribution of loads on the material. It can be written as [26]

$$K = \sigma\sqrt{\pi a} f\left(\frac{a}{W}\right). \tag{4}$$

Where $f\left(\frac{a}{W}\right)$ is a specimen geometry dependent function of the crack length a, the specimen width W, and σ is the applied stress.

In 1957, G. Irwin found that the stresses around a crack could be expressed in terms of a scaling factor called the stress intensity factor. He found that a crack subjected to any arbitrary loading could be resolved into three types of linearly independent cracking modes.[27] These load types are categorized as Mode I, II, or III as shown in the fig.13. Mode I is an opening (tensile) mode, where the crack surfaces move directly apart. Mode II is a sliding (in-plane shear) mode, where the crack surfaces slide over one another in a direction perpendicular to the leading edge of the crack. Mode III is a tearing (antiplane shear) mode, where the crack surfaces move relative to one another and parallel to the leading edge of the crack. Mode I is the most common load type encountered in engineering design.

Different subscripts are used to designate the stress intensity factor for the three different modes. The stress intensity factor for mode I is designated K_I and applied to the crack opening mode. The mode II stress intensity factor K_{II}, applies to the crack sliding mode and the mode III stress intensity factor K_{III} applies to the tearing mode. These factors are formally defined as [28]

$$\begin{aligned} K_I &= \lim_{r\to 0}\sqrt{2\pi r}\,\sigma_{yy}(r,0), \\ K_{II} &= \lim_{r\to 0}\sqrt{2\pi r}\,\sigma_{yx}(r,0), \\ K_{III} &= \lim_{r\to 0}\sqrt{2\pi r}\,\sigma_{yz}(r,0). \end{aligned} \tag{5}$$

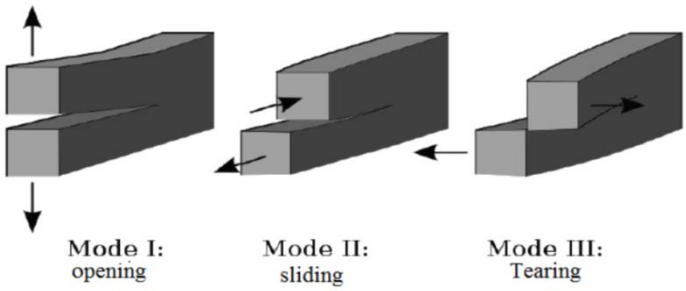

Fig.13. Schematic representation of crack loading for Mode I, Mode II and Mode III.

$$\begin{aligned} K_I &= \alpha\beta\sqrt{\pi a}, \\ \beta &= \left(1 - 0.025\alpha^2 + 0.06\alpha^4\right)\sqrt{sec\frac{\alpha\pi}{2}}, \end{aligned} \tag{6}$$

where

K_I = Stress intensity factor,

β = Geometry factor,

$\alpha = 2a/W$,

$2a$ = Crack length,

W = Width of the plate,
σ = Force applied.

Where the factor β is used to relate gross geometrical features to the stress intensity factor

$$K_I = \sigma\sqrt{\pi a}\left[\frac{1-\frac{a}{2b}+0.326\left(\frac{a}{b}\right)^2}{\sqrt{1-\frac{a}{b}}}\right]. \quad (7)$$

This study is made on a V-shaped notched plate and cracked horizontally in the middle of the notch, this plate is made of several composite materials and repaired with a V-shaped Boron/epoxy patch. The objective of this study is to evaluate the stress intensity around the crack as a function of temperature variations. Fig.14 presents similar ascending graphs for the 03 types of composites.

In the temperature range of 0°C to 40°C, the stress intensity factor values increase rapidly from 6 to 14 MPa $m^{1/2}$, but in the range [40°C-100°C], the graphs develop slightly from 14 to 18 MPa $m^{1/2}$. According to the figure, the Boron/epoxy had the lowest SIF values compared to the other types of composite with a rate of 22%.

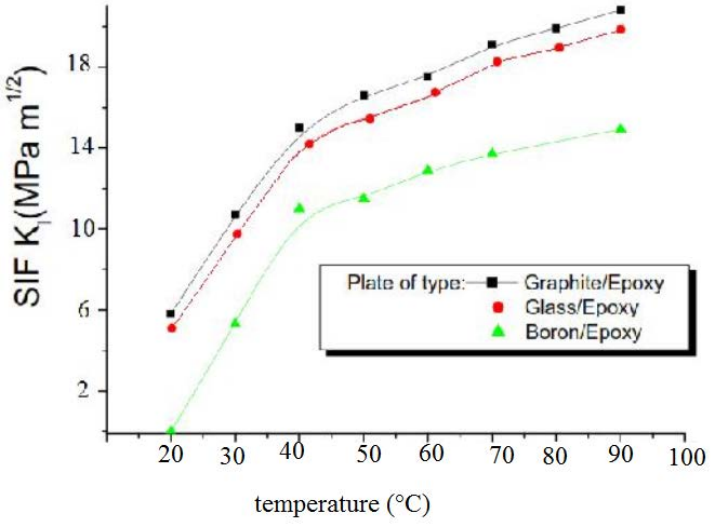

Fig.14. Variation of stress intensity factor SIF (MPa $m^{1/2}$) as a function of temperature (°C) for notched (Boron/epoxy, Graphite/epoxy and Glass/epoxy) plates and repaired with a patch (V-shaped) of boron/epoxy, FM73 adhesive.

3.2.5. Effect of patch layering.

Patch thickness is an important parameter for repairing cracked structures and improving their resistance. For this reason, fig.15 shows the effect of temperature on the SCF of a laminated boron/epoxy composite plate with a [0/45/-45/90]s stacking sequence and a patch of the same compound with a [0/45/-45/90] stacking sequence.

The stress concentration factor, K_t, is the ratio of the highest stress σ_{max} to a nominal stress σ_{nom} of the gross cross-section and defined as

$$K_t = \frac{\sigma_{max}}{\sigma_{nom}}. \quad (8)$$

Note that the dimensionless stress concentration factor is a function of the geometry shape and independent of its size. These factors can be found in typical engineering reference materials.

E. Kirsch derived the equations for the elastic stress distribution around a hole. The maximum stress felt near a hole or notch occurs in the area of lowest radius of curvature. In an elliptical hole of length 2a and width 2b, under a far-field stress σ_0, the stress at the ends of the major axes is given by Inglis' equation

$$\sigma_{max} = \sigma_0 \left(1 + 2\frac{a}{b}\right) = \left(1 + 2\sqrt{\frac{a}{\rho}}\right). \quad (9)$$

Where ρ is the radius of curvature of the elliptical hole. For circular holes in an infinite plate where $a = b$, the stress concentration factor is $K_t = 3$.

For a plate, the SCF values increase when the temperature values increase, the value of the SCF is up to 20 MPa $m^{1/2}$ at 100°C. But for the patch, the SCF values decrease slightly when the temperature rises up to 100°C. The repair effect is enhanced by a laminated patch of great mechanical and thermal resistance.

The corrective correction behavior is important in this analysis, as it is not affected by temperature rise, in contrast to the correction behavior which is affected by thermal changes, placing concentration factor values at higher pressures.

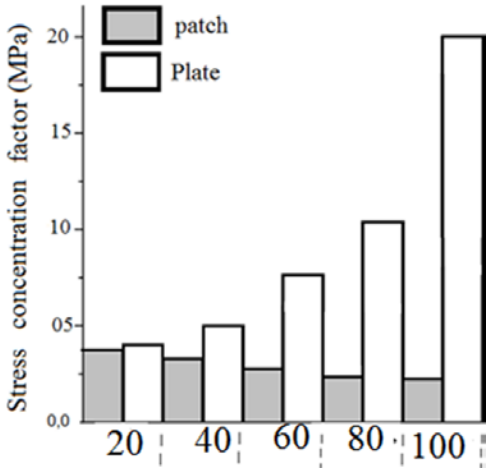

Fig.15. Influence of temperature on SCF for a [0/45/-45/90]s plate and [0/45/-45/90] patch.

4. CONCLUSION

In this work, the mechanical and thermal properties of composite materials (boron/epoxy, Glass/epoxy and graphite/epoxy) were evaluated at room temperature (20°C) and high temperatures (40, 60, 80, 100°C). This included a study in the first side, the experimental study conducted on unidirectional composite plates with different fiber orientations showed the great influence of temperature on the behavior of the composite material and its resistance to tensile strength (ultimate strength) and hardness, this experimental study proved that the increase in temperature has a negative reflection on the performance of the composite material, and it is greatly affected by temperature.

As for the modeling part, its aim was to analyze the thermal loading effect on the SIF and SCF around the crack and on the stresses distribution in the notched and cracked composite plate, where the thermal effect had a major role on the behavior

of the composite material, so that as the temperature changes increase, the intensity and concentration of stress in the composite plate increases, especially in the crack area. In addition, the composite plates and patches have a paradoxical behavior depending on the stacking sequences.

It can be concluded from the experimental and numerical study that the general mechanical properties of composite materials decrease with increasing temperature.

REFERENCES

1. Mallick P.K. *Fiber Reinforced Composites: Materials, Manufacturing and Design*. New York, Marcel Dekker Inc, 1993,584 p.
2. Aktas M. *Temperature effect on impact behavior of laminated composite plates*. Doctorate thesis, Dokuz Eylül Üniversitesi, 2007.
3. Khodja M. *The behavior of cracks repaired with composite patch en aluminium alloy 7075-T6*. Doctoral thesis. Génie mécanique Departement. D.L. Université. 2021.
4. Soutis C., Turkmen D. *Influence of shear properties and fibre imperfections on the compressive behaviour of GFRP laminates.* Applied Composite Materials, 1995, Vol.2, Pp.327-342.
5. Soutis C., Turkmen D., Morrison C.J. *Compressive Failure of Unidirectional Composites at Elevated Temperature using Untabbed Specimens*. European Conference on Composites Testing and Standardisation, ECCM-CTS 2. Hamburg, Germany, 1994, Pp.169-178.
6. El-Hawary M.M., Abdel-Fattah H. *Temperature effect on the mechanical behavior of resin concrete*. Construction and Building Materials, 2000, Vol.14, Iss.6-7, Pp.317-323.
7. Coronado P., Arguelles A., Vina J., Mollon V., Vina I. *Influence of temperature on a carbon-fibre epoxy composite subjected to static and fatique loading under mode-I delamination*. International Journal of Solids and Structures, 2012, Vol.49, Pp.2934-2940.
8. Rami A. Hawileh, Adi Abu-Obeidah, Jamel A. Abdalla, Adil Al-Tamimi. *Temperature effect on mechanical propeties of carbon, glass and carbon-glass FRP laminates*. Construction and Building Materials, 2015? Vol.75, Pp.342-348.
9. Zhongyu Lu, Guijun Xian, Hui Li. *Effects of elevated temperatures on the mechanical properties of basalt fibers and BFRP plates*. Construction and Building materials, 2016, Vol.127, Pp.1029-1036.
10. Makeev Andrew, Yihong He. *Nonlinear shear behavior and interlaminar shear strength of unidirectional polymer matrix composites: A numerical study*. International Journal of Solids and Structures, 2014, Vol.51, Pp.1263-1273.
11. Yu Bai, Thomas Keller. *Pultruded GFRP tubes with liquid-cooling system undercombined temperature and compressive loading*. Composite structures, 2009, Vol.90, 115121.
12. Botelho E.C., Pardini L.C., Rezende M.C. *Hygrothermal effects on the shear properties of carbon fiber/epoxy composites*. J. Mater Sci, 2006, Vol.41, Pp.7111-7118.
13. A. El Mourid, Ganesan R., Brochu M., Lévesque M. *Effect of temperature on the failure modes of a triaxially braided polymer matrix composite*. Int. J. Solids Struct., 2016, Vol.97-98, Pp.1-15.
14. Albedah A., Bouiadjra B.B., Mohammed S., Bnyahia F. *Fractographic anlysis*

of the overload effect on fatigue crack growth in 2024-T3 and 7075-T6 Al alloys. International Journal of Minerals Metallurgy and Materials, 2020, Vol.27, Iss.1, Pp.83-90.
15. Bercholet J.M. *Mécanique des materiaux et structures compoistes*. Lavoisier, 2010.
16. Benkhira A. *Analyse par éléments finis de la réparation des composites stratifiés endommagés par collage de patchs, thèsede doctorat*. Département Génie mécanique, Université Djilalilyabes, 2019.
17. Vu N.H., Pham X. T., François V., Cuillière J.C. *Caractérisation du comportement d'une plaque composite de grande dimension substance éts*. 2019. https://substance.etsmtl.ca/caracterisation-comportement-plaque-composite-grande-dimension# CC BY-NC 3.0.
18. Pham L., Tran P., Sanjayan J. *Steel fibres reinforced 3d printed concrete: influence of fibre sizes on mechanical performance*. Construction and Building Materials, 2020, Vol.250, 118785. https://doi.org/10.1016/j.conbuildmat.2020.118785.
19. Doo-yeol Y., Nemkumar B. *Numerical simulation on structural behavior of UHPFRC beams with steel and GFRP bars*. Computers and Concrete, 2015, Vol.16, Iss.5, Pp.759-774. https://doi.org/10.12989/cac.2015.16.5.759.
20. Gourdin S., Cormier J., Henaff G., Nadot Y., Hamon F., Pierret S. *Assessment of specific contribution of residual stress generated near surface anomalies in the high temperature fatigue life of a René 65 superalloy*. Fatigue Fracture Engineering Maters and Structures, 2016, Vol.40, Iss.1, Pp.69-80.
21. Gong X.J., Cheng P., Aivazzadeh S., Xiao X. *Design and optimisation of bonded patch repairs of laminated composite structures*. Composite Structures, 2015, Vol.123, Pp.292-300.
22. Ruoyuliu, Tao Chen, Lingzhen Li, Kazuo Tateishi. *A parctial stress intensity factor formula for CFRP repaired steel plates with a central crack*. Journal of constructional steel research, 2019, Vol.152, 105755.
23. Salem M., Berrahou M., Mechab B., Bouiadjra B.B. *Analysis of the adhesive damage for different patch shapes in bonded composite repair of corroded aluminum plate under thermo-mechanical loading*. Fail. Anal. and Preven, 2021, Vol.21, Pp.1274-1282. https://doi.org/10.1007/s11668-021-01167-x.
24. ABAQUS. ABAQUS standard/user's manual, version 6.5. HibbitKarlsson& Sorensen, Inc., Pawtucket, RI, USA, 2007.
25. Ban C.S., Lee Y.H., Choi J.H., Kweon J.H. *Strength prediction of adhesive joints using the modified damage zone theory*. Composite Structures, 2008, Vol.86, Iss.1, Pp.96-100. DOI: 10.1016/j.comp struct.03.016.
26. Janssen M., Zuidema J., Wanhill R. *Fracture mechanics*, 2nd Ed. London, 2004.
27. Suresh S. *Fatigue of Materials*. Cambridge University Press, 2004.
28. Rooke D.P., Cartwright D.J. *Compendium of stress intensity factors*. HMSO Ministry of Defence. Procurement Executive, 1976.

Received December 02, 2022.
Поступила в редакцию 02 декабря 2022 года.

Information about authors:
Сведения об авторах:
Berrahou Mohamed – Professor of Science and Technology, GIDD Laboratory, University of Relizane, Algeria; e-mail: mohamed.berrahou@univ-relizane.dz
Belkadour Leila – University of Relizane, Algeria